Environmental Science and Ecotechnology 14 (2023) 100232

Contents lists available at ScienceDirect

Environmental Science and Ecotechnology

journal homepage: www.journals.elsevier.com/environmental-science-and-ecotechnology/

Assessing the contribution of global wildfire biomass burning to BaP contamination in the Arctic

Shijie Song [a, 1], Boqi Chen [a, 1], Tao Huang [a, *], Shuxin Ma [a], Luqian Liu [a], Jinmu Luo [b, c], Huizhong Shen [d], Jiaxin Wang [a], Liang Guo [a], Min Wu [a], Xiaoxuan Mao [a], Yuan Zhao [a], Hong Gao [a], Jianmin Ma [a, e, **]

[a] Key Laboratory for Environmental Pollution Prediction and Control, Gansu Province, Key Laboratory of Western China's Environmental Systems (Ministry of Education), College of Earth and Environmental Sciences, Lanzhou University, Lanzhou, 730000, PR China
[b] Department of Earth and Atmospheric Sciences, Cornell University, Ithaca, NY, 14853, USA
[c] Department of Biological and Environmental Engineering, Cornell University, Ithaca, NY, 14853, USA
[d] School of Environmental Science and Engineering, Southern University of Science and Technology, Shenzhen, 5180551, PR China
[e] Laboratory for Earth Surface Processes, College of Urban and Environmental Sciences, Peking University, Beijing, 100871, PR China

ARTICLE INFO

Article history:
Received 2 October 2022
Received in revised form
15 December 2022
Accepted 16 December 2022

Keywords:
BaP
Arctic
Wildfires
Emissions
Source apportionment

ABSTRACT

Polycyclic aromatic hydrocarbons (PAHs) have become cause for growing concern in the Arctic ecosystems, partly due to their stable levels despite global emission reduction. Wildfire is considered one of the primary sources that influence PAH levels and trends in the Arctic, but quantitative investigations of this influence are still lacking. This study estimates the global emissions of benzo[*a*]pyrene (BaP), a congener of PAHs with high carcinogenicity, from forest and grassland fires from 2001 to 2020 and simulates the contributions of wildfire-induced BaP emissions from different source regions to BaP contamination in the Arctic. We find that global wildfires contributed 29.3% to annual averaging BaP concentrations in the Arctic from 2001 to 2020. Additionally, we show that wildfires contributed significantly to BaP concentrations in the Arctic after 2011, enhancing it from 10.1% in 2011 to 83.9% in 2020. Our results reveal that wildfires accounted for 94.2% and 50.8% of BaP levels in the Asian Arctic during boreal summer and autumn, respectively, and 74.2% and 14.5% in the North American Arctic for the same seasons. The source-tagging approach identified that local wildfire biomass emissions were the largest source of BaP in the Arctic, accounting for 65.7% of its concentration, followed by those of Northern Asia (17.8%) and Northern North America (13.7%). Our findings anticipate wildfires to play a larger role in Arctic PAH contaminations alongside continually decreasing anthropogenic emissions and climate warming in the future.

1. Introduction

Polycyclic aromatic hydrocarbons (PAHs) are an important class of organic pollutants that are primarily generated by the incomplete combustion of fossil fuels and biomass and that are ubiquitous in the global environment [1,2]. PAHs are of great public concern due to their widespread occurrence and toxic effects on ecological safety and human health [3]. PAHs released into the atmosphere tend to be adhered onto atmospheric particles, which enables them to stay in the atmosphere for a long time and undergo long-range transport (LRT) to remote locations [4,5]. Although PAHs have been regulated under the United Nations Economic Commission for Europe Aarhus Protocol on Persistent Organic Pollutants (POPs) in the Convention on Long-Range Transboundary Air Pollution (CLRTAP) [2], they can still be detected in pristine, remote areas such as the Arctic and Antarctic regions [6–14].

Given its fragile ecosystem, extensive efforts have been made to mitigate arctic environmental pollution and greenhouse gas (GHG)

* Corresponding author. Key Laboratory for Environmental Pollution Prediction and Control, Gansu Province, Key Laboratory of Western China's Environmental Systems (Ministry of Education), College of Earth and Environmental Sciences, Lanzhou University, Lanzhou, 730000, PR China.
** Corresponding author.
E-mail addresses: huangt@lzu.edu.cn (T. Huang), jmma@pku.edu.cn (J. Ma).
[1] These authors contributed equally to this work as co-first authors.

https://doi.org/10.1016/j.ese.2022.100232

emissions. As a result, most legacy POPs in the Arctic environment have declined in the past decades [2,8,15,16]. However, PAH concentrations in the Arctic showed unexpected increasing trends [2,17], despite the reduction of PAH global emissions. Studies have reported that PAH levels in Arctic fish and mussels increased 30-fold over the past 25 years [18].

Recent studies have indicated that wildland fires and global climate warming play a vital role in rising air pollution in the Arctic [19–21] so much so that wildfires have been considered a primary continental source of air pollutants [20,22,23]. Wu et al. [23] estimated that approximately 2200 tonnes of benzo[*a*]pyrene (BaP) was emitted from forest fires in 2014, accounting for 50% of global total BaP emission. Similarly, Yu et al. [2] found elevated air concentrations of phenanthrene, BaP, and pyrene at the high Arctic station of Alert from 2001 to 2005 and in 2015, which coincided with frequent summer forest fire events in the boreal forests of Canada, Alaska, and Greenland during this period, suggesting that wildfires might play a significant role in offsetting the declining trends of PAHs in the Arctic attributable to the worldwide reduction of the anthropogenic emissions. The high temperatures accompanying wildfires can also promote the re-evaporation of pollutants from the wildland and soil [22,24,25].

Although extensive investigations have been carried out to explore the source-receptor relationships of air pollution between the Arctic and worldwide emission sources using different atmospheric transport models [26–32], knowledge gaps still remain. The most significant knowledge gaps are the lack of reliable PAH emissions from wildfires and quantitative assessments of the contributions of global sources from wildfire emissions to PAH contamination in the Arctic, particularly in the most recent several years during which the Arctic and its surroundings experienced rapidly growing and severe forest fires, releasing massive amounts of GHGs and air toxics [33]. These gaps bring difficulties to understanding to what extent wildfires in the Arctic Circle and remote sources could perturb Arctic PAH contaminations.

Wang et al. [34] employed a probabilistic model based on backward air mass trajectory calculations to track sources of Arctic PAHs, and their results revealed that sources in Eastern Asia (including the Russian Far East), Europe (including European Russia), and North America account for 25%, 45%, and 27%, respectively, of the PAH atmospheric concentrations at the Alert station located in the high Canadian Arctic. Likewise, Friedman and Selin [35] estimated that more than 80% of three representatives of PAH (phenanthrene, pyrene, and BaP) atmospheric levels in the Arctic were attributable to anthropogenic emissions from Europe and Russia in 2004. However, all these studies focused on the contributions of anthropogenic PAH emissions to their level in the Arctic rather than on emissions from wildfire biomass burning.

Previous PAH emissions from wildfires have been significantly underestimated or ignored [36], such as in the EDGAR PAH emission inventory (Emissions Database for Global Atmospheric Research, https://edgar.jrc.ec.europa.eu/dataset_pop60), and this has resulted in uncertainties in estimating the impact of wildfire emission on PAH pollution in the Arctic especially. Recently, Luo et al. [20] employed carbon stock data to develop PAH emission inventory from forest fire biomass burning from 2001 to 2014, which has been shown to improve PAH emission inventory estimates significantly, and predicted BaP levels across the Arctic. However, this inventory only considered the annual mean PAH emissions from forest fire biomass burning but did not consider seasonal variation and grassland wildfire emission. Because PAH released from forest fire biomass burning may vary by orders of magnitude during different seasons, an annual emission inventory may fail to capture the seasonal changes in PAH emissions and thus lead to significant uncertainties in predicting PAH fluctuations in the Arctic.

In the present study, we develop for the first time a new global monthly BaP emission from forest and grassland biomass burning sources from 2001 to 2020 using recently updated carbon stock data up until 2020. A global atmospheric transport model, the Canadian Model for Environmental Transport of Organochlorine Pesticides (CanMETOP) [37], is then used to quantify the relative contributions of worldwide wildfire sources to BaP contaminations in the Arctic region in the past two decades. We also employ a tagging method [27] to track the long-range atmospheric transport of wildfire-biomass-burning-released BaP concentrations from 12 wildfire source regions from across the globe to the Arctic. The main objective of this study is to provide, the most comprehensive and updated assessment by far of atmospheric transport pathways of wildfire-induced PAHs from source regions to the Arctic and seasonal and interannual characteristics in the source-receptor relationships. The results may help fill knowledge gaps in the understanding of the significance of wildfires to PAH contamination in the Arctic and motivate the most appropriate response to recent international activities regarding the impact of natural emission sources on Arctic GHGs and air toxics, such as the HTAP (The Task Force on Hemispheric Transport of Air Pollution, http://htap.org/events/) under the auspices of the UNECE (the United Nations Economic Commission for Europe) Convention on Long-range Transboundary Air Pollution (CLRTAP).

2. Materials and methods

2.1. Global BaP emissions from wildfires

The term wildfire usually refers to an unplanned or unwanted fire burning in natural areas, such as forests, grasslands, or other areas [23,38], and pollutant inventories taken of these events are usually subject to high levels of uncertainty. Previous studies on PAH emissions from wildfire biomass burning considered all vegetation as a whole due to data limitations [20,23,36,39]. To improve and update wildfire-induced emission estimates of PAHs, however the wildfire biomass burning in this study is subdivided into forest and grassland fires.

The emissions of BaP were estimated using data derived from satellite products, which provided both the data related to the burned areas due to wildfire and the measured emission factors (EFs) from biomass burning. The method used to estimate wildfire emissions follows Luo et al. [20], who defined

$$E_{g,m} = \sum_{i=1}^{n} BA_{i,g,m} \times FL_{i,g,m} \times EF_i \times CE_i \quad (1)$$

where g, m, and i represent grid location, month, and vegetation type, respectively. $E_{g,m}$ represents BaP emissions from wildfire biomass burning in m at g (kg); $BA_{i,g,m}$ is the burned area in m at g for vegetation i (m^2), determined according to the intersection between vegetation areas (from Moderate Resolution Imaging Spectroradiometer (MODIS) product MCD12Q1) and burnt areas (from MODIS product MCD64CMQ) (Fig. S1); $FL_{i,g,m}$ is the aboveground carbon stock (kg m^{-2}) for vegetation type i, derived from the Global Forest Resources Assessment (https://www.fao.org/forest-resources-assessment/en/) and the MODIS satellite dataset MOD17A3H (https://lpdaac.usgs.gov/product_search/) (Fig. S2); EF_i is the emission factor of vegetation type i (Table S1); and CE_i is the combustion efficiency of vegetation type i. The wildfire emission inventory from this study extends from 2001 to 2020, with a monthly temporal resolution and 0.25° × 0.25° latitude/longitude of spatial resolution. Further details of the estimation of BaP

emission from wildfire biomass burning can be found in the Supporting Information (SI, text S1).

The uncertainty of the estimated BaP emissions in this study was quantified by calculating their 95% confidence interval (CI). The BaP emissions from wildfires were calculated as the sum of emissions from forests and grasslands, and the uncertainty of wildfire emissions was evaluated using Monte Carlo simulation [40–42]. More information about the uncertainty assessment is provided in the SI text S1 and Fig. S3.

2.2. The CanMETOP model

We used the CanMETOP to simulate the atmospheric BaP concentration and its contribution to the Arctic [37]. The CanMETOP is a three-dimensional atmospheric transport model for POPs coupled with IV-level fugacity-based multicompartment modules. We used a global scale version of the CanMETOP at a horizontal resolution of $1^\circ \times 1^\circ$ (latitude/longitude) and 14 vertical levels of 0, 1.5, 3.9, 10, 100, 350, 700, 1200, 2000, 3000, 5000, 7000, 9000, and 11000 m [43]. The six-hourly objective reanalysis data from the National Centers for Environmental Prediction Final Operational Global Analysis dataset (https://rda.ucar.edu/datasets/ds083.2) were used to provide the meteorological data to derive the CanMETOP and included winds, atmospheric pressure, temperature, and precipitation. This dataset had a spatial resolution of $1^\circ \times 1^\circ$ latitude/longitude, the same as the CanMETOP grid spacing. The six-hourly data were also interpolated into half-hourly data as the CanMETOP model integration time step length. The model topographical data, such as terrain heights and surface roughness length, were collected from the Canadian Meteorological Centre, with a spatial resolution of $1^\circ \times 1^\circ$ (latitude/longitude).

The physicochemical properties of BaP used in this simulation are presented in Table S2. The total BaP emissions, including wildfire emissions generated in this study and anthropogenic emissions covering six sectors and 69 fuel sub-types obtained from the PKU-FUEL PAH inventory database (http://inventory.pku.edu.cn/home.html), were input into the CanMETOP model as the BASE simulation. The BaP emission inventory from the wildfire biomass burning was then input into the CanMETOP model to highlight the BaP contaminations induced by wildfire biomass burning. The gridded BaP emission on $0.25^\circ \times 0.25^\circ$ latitude/longitude resolution for wildfire biomass burning and $0.1^\circ \times 0.1^\circ$ latitude/longitude resolution for anthropogenic emissions were subsequently allocated to the CanMETOP model grid on the $1^\circ \times 1^\circ$ latitude/longitude resolution. Anthropogenic BaP emissions collected from the PKU-FUEL inventory database were, however, only available through 2014. Anthropogenic emissions from 2015 to 2020 were thus assumed to be the same as in 2014, which might underestimate the impact of wildfire emissions on BaP due to a reduction in global anthropogenic PAH emissions after 2000 [36]. More detailed model descriptions can be found in previous studies [23,43,44].

2.3. The source-tagging method

A tagging method was used to trace sources of Arctic BaP pollution from its biomass burning emissions [27]. This method was previously used to quantify aerosol's source-receptor relationships without disturbing emissions. The tagging method is accurate and less computationally demanding than the widely used emission sensitivity approach [27,31,32,45]. Since the air masses between the southern and northern hemispheres seldom come in contact [31], we only focused our model on the impact of wildfire BaP emissions from 12 regions in the Northern Hemisphere (NH) (Fig. 1 and Table S3). The tagging method [27] can be defined as

$$C_{i,j} = \frac{A_{i,j}}{A_j} \quad (2)$$

where $C_{i,j}$ is the fractional contribution of the source region i to the receptor region j; $A_{i,j}$ is BaP air concentration in receptor region j that can be traced back to its source region i; and A_j is the BaP concentration in the jth receptor from all source regions defined by $A_j = \sum_i A_{i,j}$.

2.4. Model evaluation and uncertainty

Simulated BaP concentrations were compared to measured concentrations obtained from the European Monitoring and Evaluation Programme (EMEP, https://www.emep.int/), the Arctic Monitoring and Assessment Programme (AMAP, https://www.amap.no/), the Integrated Atmospheric Deposition Network (IADN, https://iadnviz.iu.edu/about/index.html), and other literature (Supplementary Data), and a significant positive correlation was observed between the simulated and measured BaP air concentration with a mean bias of -0.096 ng m^{-3}, a normalized mean bias of -18.61%, and a correlation coefficient of 0.54 (Table S4 and Fig. S4). We also compared simulated and measured site-specific changes in BaP air concentrations at three Arctic monitoring sites, Alert, Pallas, and Zeppelin (Fig. 1). Overall, the model overestimated BaP concentrations in the Arctic compared to the measured concentrations. However, the results show that the model reproduced the measured concentrations with monthly time series at three sampling sites fairly well (Fig. S4), suggesting the excellent performance of the CanMETOP model. Details of model evaluation can be found in SI (text S2, Fig. S4, and Table S4).

BaP concentrations predicted by the CanMETOP model are subject to uncertainties in input variables, including BaP emission

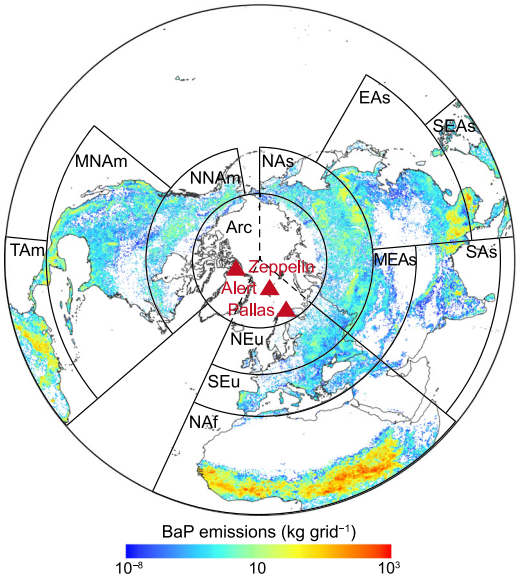

Fig. 1. The 12 selected regions in the Northern Hemisphere for source-tagging. The colors in the map represent annual mean BaP emissions from wildfires averaged from 2001 to 2020. The red triangle represents the sampling sites with time series used to compare with modeled BaP concentrations in Fig. S4c. The 12 regions are Southeast Asia (SEAs), Southern Asia (SAs), Eastern Asia (EAs), Mid-eastern Asia (MEAs), Northern Asia (NAs), Northern Africa (NAf), Southern Europe (SEu), Northern Europe (NEu), Tropical America (TAm), Middle North America (MNAm), Northern North America (NNAm), and the Arctic (Arc).

inventory, physicochemical properties, meteorological conditions, and the model representations of physical and chemical processes such as deposition, vertical transport, and degradation. Following Huang et al. [43], a first-order error propagation approach was thus employed to calculate the uncertainties in the modeled BaP concentrations [46], and the results are presented by the confidence factors (Cf) that span a 95% confidence interval. We estimate an overall uncertainty for the modeled concentration with factors of 1.87–3.29 from 2001 to 2020. Further details of the model uncertainty analysis are presented in SI text S2.

3. Results and discussions

3.1. Emissions from wildfires

The estimated annual averaging BaP emission from wildfire biomass burning from 2001 to 2020 around the globe was 2817.7 (95% CI: 1020.3–5347.3) tonnes, which is comparable to Luo et al.'s estimate [20], and it ranged from 2288.0 to 2976.3 tonnes, averaged over 2001 to 2014. Of the total wildfire emissions, forest wildfires and grassland wildfires accounted for 88.1% and 11.9% of the emissions, respectively. Figs. 1 and 2a present the spatial distributions of the annual averaging BaP emission from wildfire biomass burning in the NH from 2001 to 2020. The BaP wildfire emissions in the NH contributed approximately 30.8% of the global total wildfire emissions. Most wildfire emissions occurred in vegetation-covered areas, such as savannahs and grasslands in northern sub-Saharan Africa, forests in North America, and boreal regions in the high latitudes of Europe and Asia, where fire activities were extensive, as shown by the MCD64CMQ dataset (Fig. S1). The spatial distributions of forest-wildfire- and grassland-wildfire-induced BaP emissions are shown in Fig. 2b and c, which display a similar spatial pattern.

The temporal trend of wildfire BaP emissions in the NH from 2001 to 2020 is depicted in Fig. 3a. BaP emissions from forest fires increased from 791.7 (95% CI: 239.1–1369.9) tonnes in 2001 to a peak of 1143.4 (95% CI: 339.1–1943.1) tonnes in 2003 and declined after that to 795.7 (95% CI: 229.1–1313.1) tonnes in 2020. The grassland fire BaP emissions underwent a similar increase pattern from 74.6 (95% CI: 43.2–117.6) tonnes to 126.2 (95% CI: 55.7–152.1) tonnes from 2001 to 2003. All BaP wildfire emissions become relatively stable after 2003. Notably, the continuous decline in anthropogenic BaP emissions actually enhanced the significance of wildfire biomass BaP emission [23,36]. For example, BaP emissions from wildfires in 2014 increased by 2% from 2001. However, the anthropogenic BaP emission decreased by 26.4% during the same period. As a result, the contribution of wildfire-induced BaP emissions to the total emission around the globe increased from 34.7% in 2001 to 42.4% in 2014. Wildfires are expected to contribute significantly to global PAH emissions along with a further drop in anthropogenic emissions in the coming years due to global efforts toward PAH emission reduction.

The monthly variations in BaP wildfire emissions in the NH averaged from 2001 to 2020 are presented in Fig. 3b. As shown, wildfire-biomass-burning-induced BaP emissions in the NH occurred throughout the year, with the highest seasonal emission taking place in winter (December, January, and February), contributing 64.4% of the annual total, followed by spring (15.5%, March, April, and May), autumn (14%, September, October, and November), and summer (6.1%, June, July, and August). As shown in Fig. S5, BaP emission from wildfires in Northern Africa (including sub-Saharan Africa) dominated the total wildfire emissions in the NH, where BaP emissions were 1–2 orders of magnitude higher than from other regions (comparing the left Y-axis for emission magnitude). Researchers have demonstrated that BaP emission from forest fires in Africa alone (mostly sub-Saharan Africa) constituted 48% of the global total anthropogenic BaP emissions [23].

Significantly higher wildfires identified in tropical sub-Saharan Africa and southern and southeastern Asia mostly occurred in the NH winter and spring seasons (Fig. S5), rather than summer. The monsoon and rainy season in these regions during the summertime

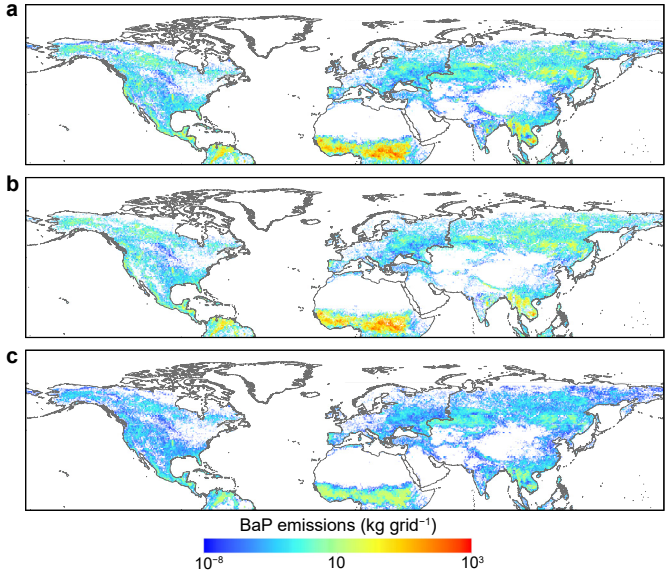

Fig. 2. Annual mean BaP emissions in the NH averaged over 2001 to 2020 for total wildfires (= forest + grass fires) (**a**), forest wildfires only (**b**), and grass wildfires only (**c**).

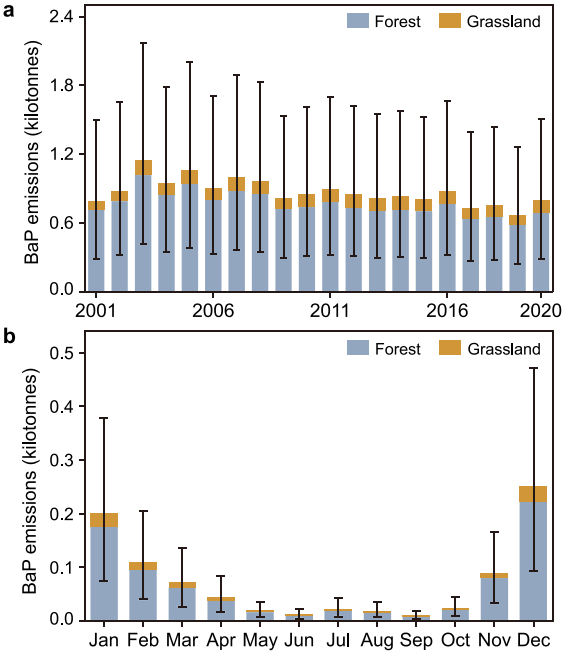

Fig. 3. **a**, Atmospheric BaP emissions from wildfire biomass burning in the NH from 2001 to 2020. **b**, Monthly BaP wildfire emissions in the NH averaged from 2001 to 2020. The error bars present a 95% confidence interval derived from first-order error propagation.

work against the occurrence of wildfires. According to the MCD64CMQ data (https://lpdaac.usgs.gov/products/mcd64a1v006/), most active fires in the NH occur in the tropics, accounting for 78% of the total area burned during 2001–2020. Moreover, forest fires determined the overall temporal trend and variation of biomass-burning-induced BaP emissions in the NH. This is because forests have a higher fuel load per unit of area burned (Fig. S2) and release more BaP to the atmosphere than grasses (Table S1). Fires in grassland, which accounted for only a small portion of BaP wildfire emissions, were relatively stable on an annual basis.

We investigated the BaP emissions from wildfire biomass burning in 12 areas in the NH. As shown in Fig. 4, overall annual variations in almost all 12 regions from 2001 to 2020 were consistent with the annual changes in wildfire-burned areas (Fig. S6). As the largest emission region, the NAf (Table S3) contributed approximately 70% to BaP emissions in the NH, but the emissions in this region decreased from 2001 to 2020 (Fig. 4). We also found larger negative slopes (trends) of linear regression relationships of annual mean wildfire-burned area against time for 2001 through 2020 (Fig. S6) that showed decreasing BaP emissions from wildfire biomass burning in the NH from 2001 to 2020 (Fig. 3a). Strong interannual fluctuations of BaP wildfire emissions occurred in most regions of the NH but without statistically significant trends. For example, large spikes of BaP emissions from wildfires frequently occurred during 2001–2020 in regions with tropical wet forests, such as TAm, SEAs, and SAs, as well as in areas with high densities of boreal forests, such as NAs, NNAm, and NEu.

The types and quantities of combustible vegetation, climatic conditions, and intensities of human activity and production vary by region, causing significant year-to-year variations in BaP emissions [47,48]. In tropical and extratropical regions, anthropogenic impacts are considered critical factors in determining fire emissions because they may increase or decrease wildfire activity through grazing, clearing forests, altering ignition patterns, and suppressing fires. The same decreasing trends in wildfire emissions in NAf have also been identified in other studies [49,50]. Wu et al. [50] suggested that the decline in the burning area in Africa was likely associated with the expansion of high-capital agriculture.

We also observed that the BaP wildfire emissions in TAm increased from 2001 to 2003 and decreased from 2003 to 2012. From 2012 onward, the wildfire emissions increased again through 2020. Wildfire severity in the Arctic significantly increased in the first two decades of the 21st century [51,52]. From 2001 to 2010 and from 2011 to 2020, the burned area increased by a factor of approximately 3, corresponding to a doubling of the BaP emissions from wildfire. This increase in wildfire-induced BaP emissions was also consistent with the increased wildfire pattern in the Siberian taiga and the tundra in Alaska and Canada since the 2000s [51,53].

Monthly mean BaP emissions from wildfire biomass burning in 12 regions in the NH averaged over 2001 to 2020 are shown in Fig. S5. The BaP emissions from wildfire biomass burning fluctuated monthly, with a high frequency of change occurring in the warm season (June–August) in the regions of SEu, the Arctic, NNAm, MEAs, and NAs, and in the dry months (January–April, and December) for NEu, TAm, NAf, SAs, SEAs, and EAs. Moreover, grassland wildfires contributed to more BaP emissions in Mid-East Asia than forest wildfires due to higher grassland cover in this region.

3.2. Ambient BaP air concentrations from wildfire emissions

To quantify contributions of worldwide wildfire emissions to BaP contamination in the Arctic, we simulated BaP air concentrations from 2001 to 2020 from all emission sources and wildfire sources only in the Arctic. Ambient BaP air concentrations simulations from all sources are presented in SI (text S3 and Fig. S7). Fig. S8a shows the modeled annually averaged daily BaP air concentrations over the Arctic from 2001 to 2020 derived from wildfire emissions. The annually averaged daily BaP concentrations from

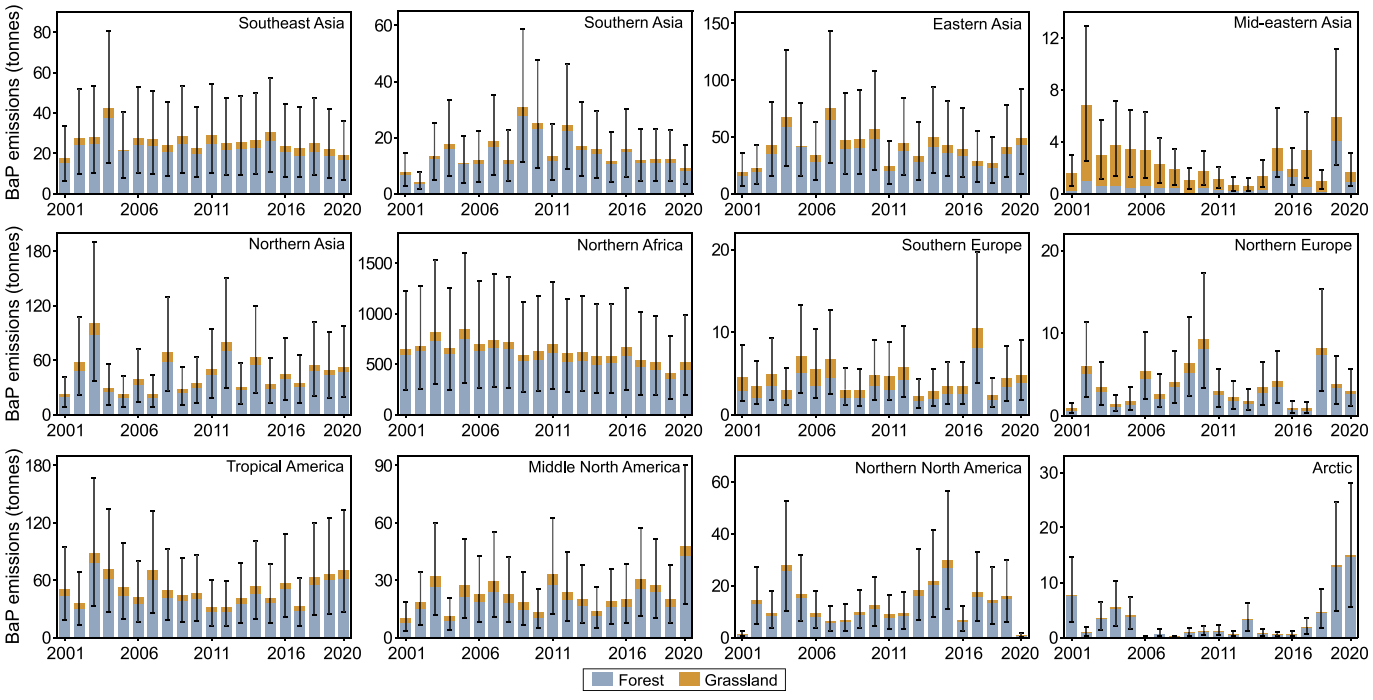

Fig. 4. Annual BaP emissions from wildfire biomass burning in 12 regions from 2001 to 2020. The error bars present a 95% confidence interval derived from the first-order error propagation.

2001 to 2020 across the Arctic ranged from 10^{-6} (95% CI: 4.7×10^{-7}–2.1×10^{-6}) pg m^{-3} to 161.8 (95% CI: 76.3–343.1) pg m^{-3}, with a mean concentration of 0.9 (95% CI: 0.4–1.9) pg m^{-3}, which is equivalent to about one-third of the annual mean BaP air concentrations of 2.9 (95% CI: 1.2–6.8) pg m^{-3} predicted using all emissions sources (anthropogenic + wildfire) in the Arctic (Fig. S7). Higher BaP air concentrations were seen in Alaska, northern Canada, and Siberia. We classified the area north of 66.5° N, 30° W–50° E as the European Arctic, the area from 50° E to 180° E as the Asian (including Eastern Russia) Arctic, and the area from 180° E to 30° W as the North American Arctic. Our results show that the Asian Arctic suffered from the heaviest BaP contamination, with an average concentration of 1.7 (95% CI: 0.8–3.6) pg m^{-3}, followed by the North American Arctic (0.6, 95% CI: 0.3–1.3 pg m^{-3}), and European Arctic (0.01, 95% CI: 0.005–0.02 pg m^{-3}).

We further examined the temporal variation of BaP concentrations from the wildfire emissions over the Arctic from 2001 to 2020 (Fig. S8b). The results reveal fluctuating BaP air concentrations in the Arctic from 2001 onward but increasing rapidly after 2016. The decadal mean BaP concentration from wildfire emissions almost doubled from the 2001–2010 (0.6, 95% CI: 0.3–1.3 pg m^{-3}) to the 2011–2020 period (1.0, 95% CI: 0.5–2.1 pg m^{-3}). However, this BaP concentration increase was not geographically uniform. The greatest increase in BaP concentrations occurred in the Asian Arctic (Fig. S8c) but this concentration actually decreased during 2011–2020 in the North American Arctic (Fig. S8d). The highest annual BaP concentration in the European Arctic occurred in 2018 (Fig. S8e). However, this peak concentration value did not significantly disturb the mean BaP concentrations in the entire Arctic because of considerably lower concentrations in the European Arctic compared to other Arctic regions.

Partly due to much faster warming in the Arctic than in the rest of the world [54–56], Arctic wildfires occurred more frequently in recent decades [51], causing significantly elevated BaP emissions (Fig. 4) and air concentrations (Fig. S8b), especially increasing annual BaP concentrations after 2016 that were associated with extremes in air temperature [51,52]. In particular, the annual mean air concentration of BaP in 2020 was 1.3–57.9 times higher than previous years, accompanied by the highest air temperatures ever recorded [57,58]. In addition, the highest BaP air concentrations from 2001 to 2020 were found in summer (2.3, 95% CI: 1.1–4.8 pg m^{-3}), followed by autumn (0.6, 95% CI: 0.3–1.2 pg m^{-3}), spring (0.4, 95% CI: 0.2–0.7 pg m^{-3}), and winter (0.2, 95% CI: 0.1–0.3 pg m^{-3}) (Figs. S9 and S10).

3.3. Tagging wildfire emission sources of BaP pollution in the Arctic

The contribution of emissions from wildfire sources across the NH to the annual BaP air concentrations from all emission (anthropogenic + natural) sources in the Arctic from 2001 to 2020 is depicted in Fig. 5a. The most significant contribution was observed in Alaska, Siberia, and Canada's Yukon and Northwest Territories, where wildfires contributed nearly 90% to BaP concentrations. Overall, BaP wildfire emissions are estimated to have contributed about 29.3% to the BaP concentrations from all sources over the Arctic, 56.6% to the Asian Arctic, 37.7% to the American Arctic, and 0.4% to the European Arctic.

The relative contributions of natural wildfire emissions to the annual mean BaP air concentrations from all sources in the pan-Arctic region from 2001 to 2020 are shown in Fig. 5b–e. The source contributions to BaP air concentrations fluctuated markedly due to significant interannual variation of wildfire emissions. Our results reveal that the contributions from wildfire-induced emissions to all source-generated BaP concentrations in the Arctic exhibited an increasing trend from 24.6% in 2001 to 33.9% in 2005. From 2006 to 2012, the contributions from wildfire emissions were lower than 20% but significant changes occurred after 2012. The contribution from the wildfire emissions rapidly increased to 83.9% in 2020, with an annual growth rate of 8.5%. In contrast, the contribution in three sub-regions exhibited considerable interannual variation.

We also examined the monthly variations in the contributions from wildfire emissions to BaP air concentrations in the Arctic (Fig. S11) and found that the most significant contribution of wildfire emissions to BaP levels in the Arctic occurred in summer (68.0%), followed by autumn (12.7%), spring (5.3%), and winter

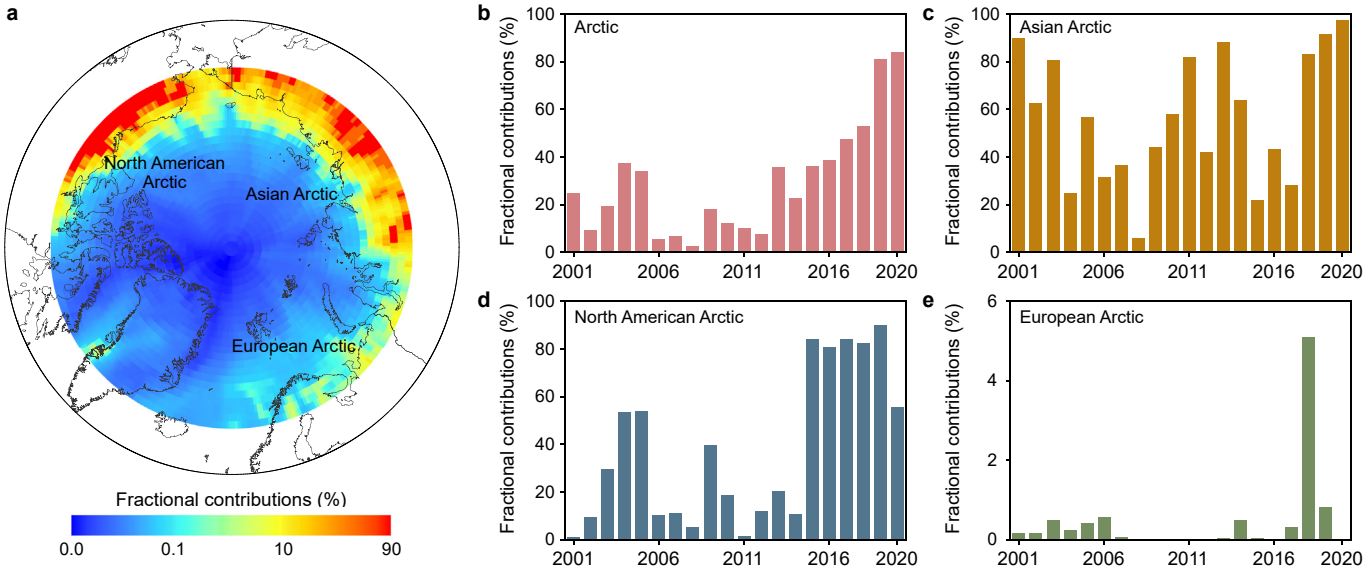

Fig. 5. Fractional contributions of wildfire emissions to BaP air concentrations. **a**, Fractional contribution (%) of wildfire emissions to BaP air concentrations averaged over the Arctic from 2001 to 2020. **b**–**e**, Annual variation of the contribution of wildfire emissions to BaP concentrations from 2001 to 2020 in the Arctic (**b**), the Asian Arctic (**c**), the North American Arctic (**d**), and the European Arctic (**e**). The fractional contribution is defined as $(C_{wildfire}/C_{base}) \times 100$, where $C_{wildfire}$ and C_{base} are BaP air concentrations simulated by the CanMETOP model subject to wildfire and total BaP emissions.

(1.6%). The weak contribution from wildfire emissions to BaP air pollution in the wintertime could be attributed to low forest and grass fire activities in the high latitude regions (boreal forests), and the significantly higher contributions from wildfire emissions to summer and autumn BaP contaminations in the Arctic were associated with the warm season's high burning frequency in the boreal forests proximate to the pan-Arctic region. The wildfires during these two seasons accounted for 94.2% and 50.8% of BaP concentrations in the Asian Arctic and 74.2% and 14.5% in the North American Arctic, respectively.

Overall, our results reveal that the interannual and monthly variations of BaP contaminations in the Arctic caused by wildfire emissions were significantly higher than those of anthropogenic emissions, especially during periods with significantly high frequency of wildfires. As shown in Fig. 5, our updated BaP emission inventory from wildfires and modeled BaP concentrations across the Arctic capture nicely the unprecedented amount of wildfires that occurred in the Arctic in the spring and summer of 2019 and 2020, characterized by significantly rising emissions and air concentrations.

Due to the significant contribution of wildfires to BaP contamination in the Arctic, we further explored the influences of wildfires that occurred in the specified source regions (Fig. S12a and Table S3) on the Arctic BaP concentrations using the source tagging technique. Fig. S12 illustrates the BaP air concentrations in the Arctic from 2001 to 2020 derived from wildfire-biomass-burning-induced emissions from different source regions. The results show that the pan-Arctic local wildfire emissions contributed 38.2–70.1% to BaP concentrations in the entire Arctic and the different Arctic regions (Asian Arctic, North American Arctic, and European Arctic) from 2001 to 2020. The nonlocal wildfire emission sources in NAs, NNAm, and NEu (Fig. S12a and Table S3) contributed 28.5%, 0.1%, and 0.3% to airborne BaP in the Asian Arctic, 4.1%, 35.3%, and 0.2% to the North American Arctic, and 3.6%, 4.5%, and 44.3% to the European Arctic, respectively. Fig. 6 also shows the spatial distribution of BaP concentrations from wildfire biomass burning from each source region. The local Arctic wildfire emissions were confined within the high latitudes and hence made the largest contributions to the BaP air concentrations, notably near the sources in northern Canada and the Russian Arctic. Airborne BaP from NAs and NNAm sources were readily delivered to the Arctic via poleward air flows from Siberia and Greenland. The prevailing

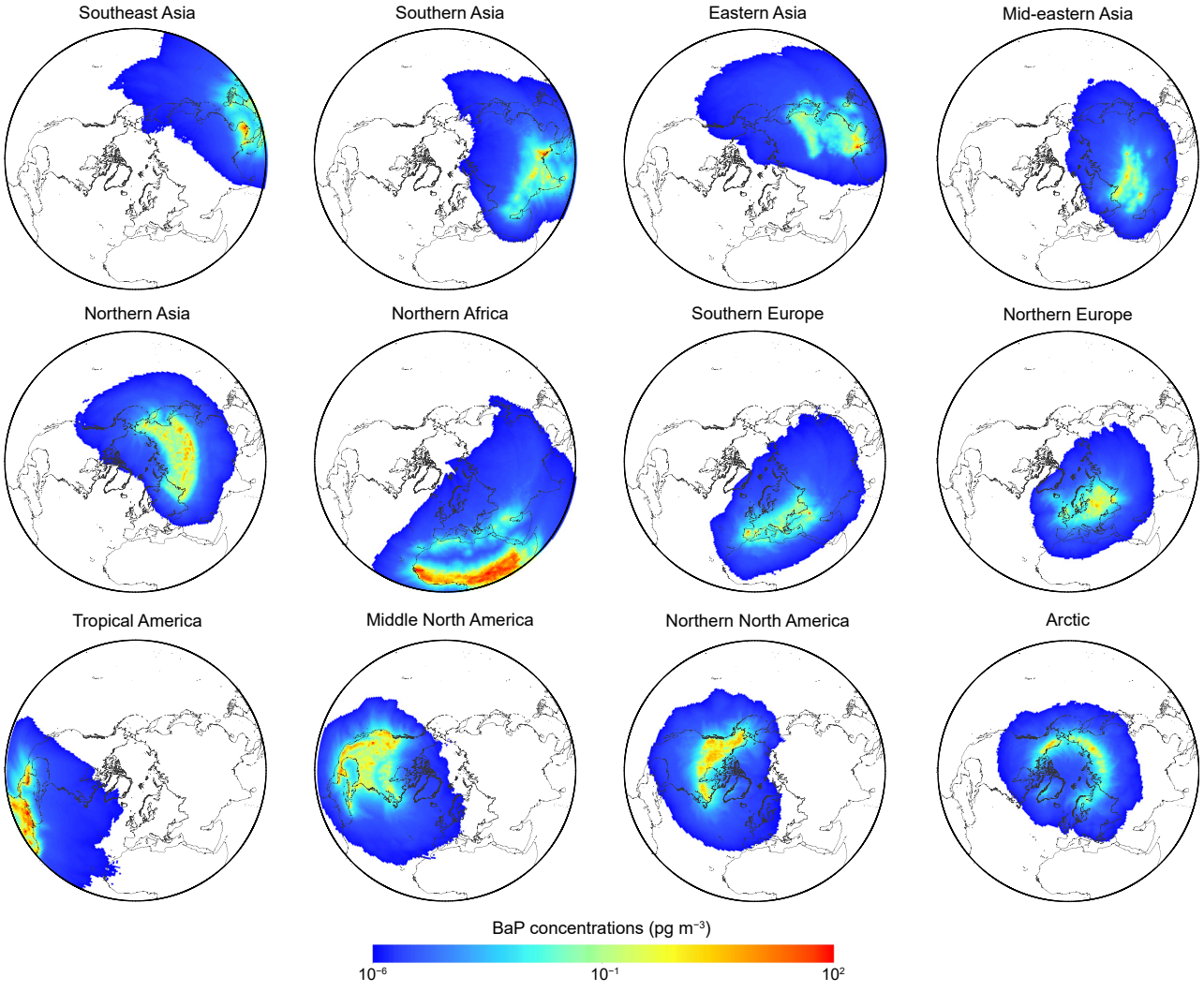

Fig. 6. The spatial distribution of modeled annually averaged daily BaP air concentration over Arctic averaged over 2001 to 2020 subject to BaP wildfire biomass burning emissions in each of the 12 regions.

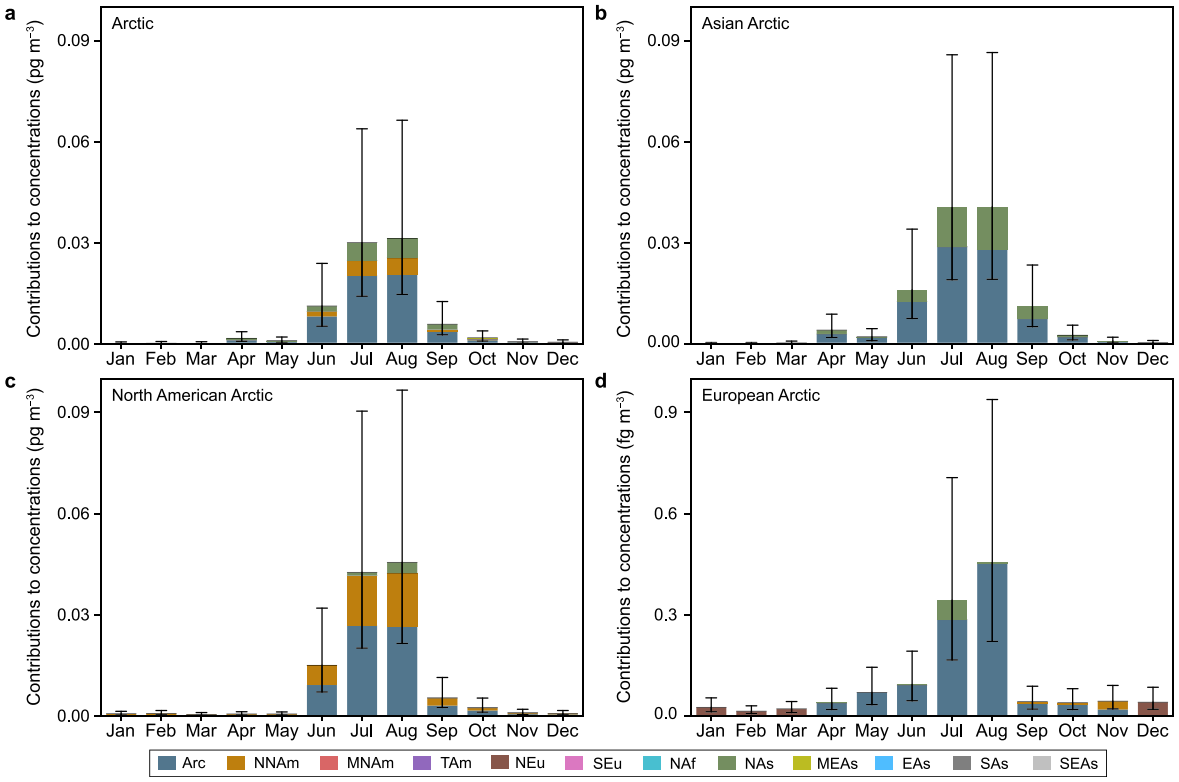

Fig. 7. Monthly-averaged BaP concentrations from wildfire biomass burning in 12 regions from 2001 to 2020 in the entire Arctic (**a**), the Asian Arctic (**b**), the North American Arctic (**c**), and the European Arctic (**d**). The error bars present a 95% confidence interval derived from first-order error propagation.

westerly flows at the free troposphere in the NH also provided pathways for the wildfire emissions derived airborne BaP from NNAm, SEu, MEAs, and EAs to the Arctic [59–61]. In contrast, although the NAf was the largest wildfire BaP emission source, the remoteness of this source region to the Arctic yields a very small, if not negligible, contribution to the airborne BaP in the polar region.

We also examined the monthly contributions from the NH regional wildfire emissions to BaP air concentrations in the Arctic (Fig. 7) and found that the airborne BaP pollution in the Arctic associated with nonlocal wildfire emission sources occurred mainly in the summer months (June, July, and August). In particular, two primary non-local source regions, wildfire sources in NAs and NNAm contributed 17.4% and 14.9% to the airborne BaP in the entire Arctic, 30.1% and 0.1% in the Asian Arctic, and 4.5% and 35.4% in the Northern American Arctic during the summer season, respectively.

4. Conclusions

In this study, we developed a unique and most-comprehensive-to-date gridded global BaP wildfire emission inventory that takes both forest and grass fires into consideration. The inventory was implemented into an atmospheric transport model (CanMETOP) to assess the impacts of global wildfire emissions on Arctic BaP contamination from 2001 to 2020 systemically and quantitatively. The modeling results show that the wildfire emissions in the NH contributed 29.3% to annually averaged BaP concentration over the Arctic from 2001 to 2022, respectively. Our results also reveal that wildfire emissions played an increasingly vital role in BaP contamination in the past decade in the Arctic, which enhanced the contribution of wildfire emissions to airborne BaP in the polar region from 10.1% in 2011 to 83.9% in 2020. Source proximity also played a crucial role in the wildfire-emission-derived airborne BaP in the Arctic. However, these nearby sources, such as NAs and NNAm, also contributed about 28.5% to BaP concentrations in the Asian Arctic and 35.4% in the North American Arctic. We further showed that the BaP global wildfire emission inventory and modeling results successfully captured rapidly increasing BaP concentrations associated with the unprecedented wildfires that occurred in the Arctic and its vicinity in 2019 and 2020 [62].

The Arctic is projected to continue warming [63,64], and we would expect increasing wildfire events in the polar and high latitude regions due to more rapid warming in these regions than low latitude regions. As a result, wildfire emissions might increasingly contribute to the contamination levels of toxic chemicals across the Arctic, along with declining anthropogenic emissions under global mitigation of GHG and efforts to improve air quality. In light of this, our study helps to fill knowledge gaps in understanding the source-receptor relationships of air pollutants in the Arctic and their associations with climate change. The results also provide a reference to policymakers and stakeholders to guide strategies and responses to wildfire-induced GHG and toxic air emissions, which would overwhelm anthropogenic emissions in the Arctic in the future.

CRediT author contribution statement

Shijie Song: methodology, formal analysis, investigation, writing, review and editing; **Boqi Chen:** methodology, formal analysis, investigation, writing, review and editing; **Tao Huang:** conceptualization, methodology, investigation, supervision, writing, review, editing, and funding acquisition; **Shuxin Ma:** methodology, data curation, validation; **Luqian Liu:** data curation, validation, and software; **Jinmu Luo:** investigation and data curation; **Huizhong Shen:** investigation and data curation; **Jiaxin**

Wang: data curation and validation; **Liang Guo:** validation and software; **Min Wu:** validation; **Xiaoxuan Mao:** data curation; **Yuan Zhao:** software; **Hong Gao:** supervision and funding acquisition; **Jianmin Ma:** conceptualization, methodology, investigation, supervision, writing, review, editing, and funding acquisition.

Declaration of competing interests

The authors declare that they have no known competing financial interests or personal relationships that could have appeared to influence the work reported in this paper.

Acknowledgments

We acknowledge the free use of gridded global anthropogenic BaP emissions data from Peking University. This research was supported by the National Natural Science Foundation of China through grants 41877507, 41977357, and 42177351.

Appendix A. Supplementary data

Supplementary data to this article can be found online at https://doi.org/10.1016/j.ese.2022.100232.

References

[1] C.L. Friedman, Y.X. Zhang, N.E. Selin, Climate change and emissions impacts on atmospheric PAH transport to the Arctic, Environ. Sci. Technol. 48 (1) (2014) 429–437, https://doi.org/10.1021/es403098w.
[2] Y. Yu, A. Katsoyiannis, N.P. Bohlin, E. Brorström-Lundén, J.M. Ma, Y. Zhao, Z.Y. Wu, W. Tych, D. Mindham, E. Sverko, E. Barresi, H. Dryfhout-Clark, P. Fellin, H. Hung, Polycyclic aromatic hydrocarbons not declining in Arctic air despite global emission reduction, Environ. Sci. Technol. 53 (2019) 2375–2382, https://doi.org/10.1021/acs.est.8b05353.
[3] B. Aichner, B. Bussian, P. Lehnik-Habrink, S. Hein, Levels and spatial distribution of persistent organic pollutants in the environment: a case study of German forest soils, Environ. Sci. Technol. 47 (22) (2013) 12703–12714, https://doi.org/10.1021/es4019833.
[4] D.C.G. Muir, E. Galarneau, Polycyclic aromatic compounds (PACs) in the Canadian environment: links to global change, Environ. Pollut. 273 (2021), 116425, https://doi.org/10.1016/j.envpol.2021.116425.
[5] S. Zhou, A.K.Y. Lee, R.D. McWhinney, J.P.D. Abbatt, Burial effects of organic coatings on the heterogeneous reactivity of particle-borne benzo[a]pyrene (BaP) toward ozone, J. Phys. Chem. A 116 (2012) 7050–7056, https://doi.org/10.1021/jp3030705.
[6] Z. Wang, G.S. Na, X.D. Ma, L.K. Ge, Z.S. Lin, Z.W. Yao, Characterizing the distribution of selected PBDEs in soil, moss and reindeer dung at Ny-Alesund of the Arctic, Chemosphere 137 (2015) 9–13, https://doi.org/10.1016/j.chemosphere.2015.04.030.
[7] M. Jin, J. Fu, B. Xue, S. Zhou, L. Zhang, A. Li, Distribution and enantiomeric profiles of organochlorine pesticides in surface sediments from the Bering Sea, Chukchi Sea and adjacent Arctic areas, Environ. Pollut. 222 (2017) 109–117, https://doi.org/10.1016/j.envpol.2016.12.075.
[8] F. Wong, H. Hung, H. Dryfhout-Clark, W. Aas, P. Bohlin-Nizzetto, K. Breivik, M.N. Mastromonaco, E.B. Lundén, K. Ólafsdóttir, Á. Sigurðsson, K. Vorkamp, R. Bossi, H. Skov, H. Hakola, E. Barresi, E. Sverko, P. Fellin, H. Li, A. Vlasenko, M. Zapevalov, D. Samsonov, S. Wilson, Time trends of persistent organic pollutants (POPs) and Chemicals of Emerging Arctic Concern (CEAC) in Arctic air from 25 years of monitoring, Sci. Total Environ. 775 (2021), 145109, https://doi.org/10.1016/j.scitotenv.2021.145109.
[9] Arctic Monitoringand Assessment Programme (AMAP), AMAP assessment 2015: temporal trends in persistent organic pollutants in the arctic. https://www.amap.no/documents/doc/AMAP-Assessment-2015-Temporal-Trends-in-Persistent-Organic-Pollutants-in-the-Arctic/1521. (Accessed August 2022).
[10] J. Balmer, H. Hung, Y. Yu, R.J. Letcher, D.C.G. Muir, Sources and environmental fate of pyrogenic polycyclic aromatic hydrocarbons (PAHs) in the Arctic, Emerg. Contam. 5 (2019) 128–142, https://doi.org/10.1016/j.emcon.2019.04.002.
[11] X. Wang, C. Wang, T. Zhu, P. Gong, J. Fu, Z. Cong, Persistent organic pollutants in the polar regions and the Tibetan Plateau: a review of current knowledge and future prospects, Environ. Pollut. 248 (2019) 191–208, https://doi.org/10.1016/j.envpol.2019.01.093.
[12] A. Cabrerizo, D.C.G. Muir, G. Kock, D. Iqaluk, X. Wang, Climatic influence on temporal trends of polychlorinated biphenyls and organochlorine pesticides in landlocked char from lakes in the Canadian high arctic, Environ. Sci. Technol. 52 (2018) 10380–10390, https://doi.org/10.1021/acs.est.8b01860.
[13] P.J. Lewis, A. Lashko, A. Chiaradia, G. Allinson, J. Shimeta, L. Emmerson, New and legacy persistent organic pollutants (POPs) in breeding seabirds from the East Antarctic, Environ. Pollut. 309 (2022), 119734, https://doi.org/10.1016/j.envpol.2022.119734.
[14] Z. Xie, P. Zhang, Z. Wu, S. Zhang, L. Wei, L. Mi, A. Kuester, J. Gandrass, R. Ebinghaus, R. Yang, Z. Wang, W. Mi, Legacy and emerging organic contaminants in the polar regions, Sci. Total Environ. 835 (2022), 155376, https://doi.org/10.1016/j.scitotenv.2022.155376.
[15] H. Hung, A.A. Katsoyiannis, E. Brorström-Lundén, K. Olafsdottir, W. Aas, K. Breivik, P. Bohlin-Nizzetto, A. Sigurdsson, H. Hakola, R. Bossi, Temporal trends of persistent organic pollutants (POPs) in arctic air: 20 years of monitoring under the arctic monitoring and assessment Programme (AMAP), Environ. Pollut. 217 (2016) 52–61, https://doi.org/10.1016/j.envpol.2016.01.079.
[16] P. Anttila, E. Brorström-Lundén, K. Hansson, H. Hakola, M. Vestenius, Assessment of the spatial and temporal distribution of persistent organic pollutants (POPs) in the Nordic atmosphere, Atmos. Environ. 140 (2016) 22–33, https://doi.org/10.1016/j.atmosenv.2016.05.044.
[17] H. Hung, C. Halsall, H. Ball, T. Bidleman, J. Dachs, A. De Silva, M. Hermanson, R. Kallenborn, D. Muir, R. Suhring, X. Wang, S. Wilson, Climate change influence on the levels and trends of persistent organic pollutants (POPs) and chemicals of emerging Arctic concern (CEACs) in the Arctic physical environment – a review, Environ. Sci. Processes Impacts (2022), https://doi.org/10.1039/D1EM00485A.
[18] F.D. Laender, J. Hammer, A.J. Hendriks, K. Soetaert, C.R. Janssen, Combining monitoring data and modeling identifies PAHs as emerging contaminants in the Arctic, Environ. Sci. Technol. 45 (20) (2011) 9024–9029, https://doi.org/10.1021/es202423f.
[19] J. Ma, H. Hung, R.W. Macdonald, The influence of global climate change on the environmental fate of persistent organic pollutants: a review with emphasis on the Northern Hemisphere and the Arctic as a receptor, Global Planet. Change 146 (2016) 89–108, https://doi.org/10.1016/j.gloplacha.2016.09.011.
[20] J. Luo, Y. Han, Y. Zhao, Y. Huang, X. Liu, S. Tao, J. Liu, T. Huang, L. Wang, K. Chen, J. Ma, Effect of northern boreal forest fires on PAH fluctuations across the Arctic, Environ. Pollut. 261 (2020), 114186, https://doi.org/10.1016/j.envpol.2020.114186.
[21] Y. Zhao, L. Wang, J. Luo, T. Huang, S. Tao, J. Liu, Y. Yu, Y. Huang, X. Liu, J. Ma, Deep learning prediction of polycyclic aromatic hydrocarbons in the high Arctic, Environ. Sci. Technol. 53 (2019) 13238–13245, https://doi.org/10.1021/acs.est.9b05000.
[22] P. Gong, X.P. Wang, Forest fires enhance the emission and transport of persistent organic pollutants and polycyclic aromatic hydrocarbons from the Central Himalaya to the Tibetan Plateau, Environ. Sci. Technol. Lett. 8 (2021) 498–503, https://doi.org/10.1021/acs.estlett.1c00221.
[23] M. Wu, J.M. Luo, T. Huang, L.L. Lian, T.L. Chen, S.J. Song, Z.X. Wang, S.X. Ma, C.R. Xie, Y. Zhao, X.X. Mao, H. Gao, J.M. Ma, Effects of African BaP emission from wildfire biomass burning on regional and global environment and human health, Environ. Int. 162 (2022), 107162, https://doi.org/10.1016/j.envint.2022.107162.
[24] X. Wang, C.P. Meyer, F. Reisen, M. Keywood, P.K. Thai, D.W. Hawker, J. Powell, J.F. Mueller, Emission factors for selected semivolatile organic chemicals from burning of tropical biomass fuels and estimation of annual Australian emissions, Environ. Sci. Technol. 51 (17) (2017), https://doi.org/10.1021/acs.est.7b01392, 9644–9652.
[25] G. Lammel, C. Degrendele, S.S. Gunthe, Q. Mu, A. Muthalagu, O. Audy, C.V. Biju, P. Kukucka, M.D. Mulder, M. Octaviani, P. Příbylová, P. Shahpoury, I. Stemmler, A.E. Valsan, Revolatilisation of soil-accumulated pollutants triggered by the summer monsoon in India, Atmos. Chem. Phys. 18 (15) (2018) 11031–11040, https://doi.org/10.5194/acp-18-11031-2018.
[26] S. Sharma, M. Ishizawa, D. Chan, D. Lavoué, E. Andrews, K. Eleftheriadis, S. Maksyutov, 16-year simulation of Arctic black carbon: transport, source contribution, and sensitivity analysis on deposition, J. Geophys. Res. Atmos. 118 (2013) 943–964, https://doi.org/10.1029/2012JD017774.
[27] H. Wang, P.J. Rasch, R.C. Easter, B. Singh, R. Zhang, P.-L. Ma, Y. Qian, S.J. Ghan, N. Beagley, Using an explicit emission tagging method in global modeling of source-receptor relationships for black carbon in the Arctic: variations, sources, and transport pathways, J. Geophys. Res. Atmos. 119 (2014), https://doi.org/10.1002/2014JD022297 (2014) 888–12,909.
[28] A. Kumar, S. Wu, Mercury pollution in the arctic from wildfires: source attribution for the 2000s, Environ. Sci. Technol. 53 (2019) 11269–11275, https://doi.org/10.1021/acs.est.9b01773.
[29] J.E. Balmer, H. Hung, Y. Yu, R.J. Letcher, D.C.G. Muir, Sources and environmental fate of pyrogenic polycyclic aromatic hydrocarbons (PAHs) in the Arctic, Emerg. Contam. 5 (2019) 128–142, https://doi.org/10.1016/j.emcon.2019.04.002.
[30] K. Ikeda, H. Tanimoto, T. Sugita, H. Akiyoshi, Y. Kanaya, C. Zhu, F. Taketani, Tagged tracer simulations of black carbon in the Arctic: transport, source contributions, and budget, Atmos. Chem. Phys. 17 (2017) 10515–10533, https://doi.org/10.5194/acp-17-10515-2017, 2017.
[31] H. Matsui, T. Mori, S. Ohata, N. Moteki, N. Oshima, K. Goto-Azuma, M. Koike, Y. Kondo, Contrasting source contributions of Arctic black carbon to atmospheric concentrations, deposition flux, and atmospheric and snow radiative effects, Atmos. Chem. Phys. 22 (2022) 8989–9009, https://doi.org/10.5194/acp-22-8989-2022.
[32] L. Ren, Y. Yang, H. Wang, R. Zhang, P. Wang, H. Liao, Source attribution of Arctic black carbon and sulfate aerosols and associated Arctic surface

warming during 1980–2018, Atmos. Chem. Phys. 20 (2020) 9067–9085, https://doi.org/10.5194/acp-20-9067-2020.
[33] A. Witze, The Arctic is burning like never before — and that's bad news for climate change, Nature 585 (2020) 336–337, https://doi.org/10.1038/d41586-020-02568-y.
[34] R. Wang, S. Tao, B. Wang, Y. Yang, C. Lang, Y. Zhang, J. Hu, J. Ma, H. Hung, Sources and pathways of polycyclic aromatic hydrocarbons transported to Alert, the Canadian High Arctic, Environ. Sci. Technol. 44 (3) (2010) 1017–1022, https://doi.org/10.1021/es902203w.
[35] C.L. Friedman, N.E. Selin, Long-range atmospheric transport of polycyclic aromatic hydrocarbons: a global 3-D model analysis including evaluation of Arctic sources, Environ. Sci. Technol. 46 (2012) 9501–9510, https://doi.org/10.1021/es301904d.
[36] H.Z. Shen, Y. Huang, R. Wang, D. Zhu, W. Li, G.F. Shen, B. Wang, Y.Y. Zhang, Y.C. Chen, Y. Lu, H. Chen, T.C. Li, K. Sun, B.G. Li, W.X. Liu, J.F. Liu, S. Tao, Global atmospheric emissions of polycyclic aromatic hydrocarbons from 1960 to 2008 and future predictions, Environ. Sci. Technol. 47 (2013) 6415–6424, https://doi.org/10.1021/es400857z.
[37] J. Ma, S. Daggupaty, T. Harner, Y. Li, Impacts of lindane usage in the Canadian prairies on the Great Lakes ecosystem. 1. Coupled atmospheric transport model and modeled concentrations in air and soil, Environ. Sci. Technol. 37 (17) (2003) 3774–3781, https://doi.org/10.1021/es034160x.
[38] The Federal Emergency Management Agency, Wildfire. https://community.fema.gov/ProtectiveActions/s/article/Wildfire-What. (Accessed July 2022).
[39] Y. Zhang, S. Tao, Global atmospheric emission inventory of polycyclic aromatic hydrocarbons (PAHs) for 2004, Atmos. Environ. 43 (2009) 812–819, https://doi.org/10.1016/j.atmosenv.2008.10.050.
[40] Y. Xu, C. Tian, J. Ma, X. Wang, J. Li, J. Tang, Y. Chen, W. Qin, G. Zhang, Assessing cancer risk in China from γ-hexachlorocyclohexane emitted from Chinese and Indian sources, Environ. Sci. Technol. 47 (2013) 7242–7249, https://doi.org/10.1021/es400141e.
[41] H.R. Xu, Y.A. Ren, W.X. Zhang, W.J. Meng, X. Yun, X.Y. Yu, J. Li, Y.Z. Zhang, G.F. Shen, J.M. Ma, B.G. Li, H.F. Cheng, X.L. Wang, Y. Wan, S. Tao, Updated global black carbon emissions from 1960 to 2017: improvements, trends, and drivers, Environ. Sci. Technol. 55 (2021), https://doi.org/10.1021/acs.est.1c03117, 7869–7879.
[42] B.Q. Zhang, H.Z. Shen, X. Yun, Q.R. Zhong, B.H. Henderson, X. Wang, L.H. Shi, S.S. Gunthe, L.G. Huey, S. Tao, A.G. Russell, P.F. Liu, Global emissions of hydrogen chloride and particulate chloride from continental sources, Environ. Sci. Technol. 56 (7) (2022), https://doi.org/10.1021/acs.est.1c05634, 3894–3904.
[43] T. Huang, Z. Ling, J. Ma, R.W. Macdonald, H. Gao, S. Tao, C. Tian, S. Song, W. Jiang, L. Chen, K. Chen, Z. Xie, Y. Zhao, L. Zhao, C. Gu, X. Mao, Human exposure to polychlorinated biphenyls embodied in global fish trade, Nature Food 1 (5) (2020) 292–300, https://doi.org/10.1038/s43016-020-0066-1.
[44] W.Y.H. Jiang, T. Huang, X.X. Mao, W. Li, Y. Zhao, C.H. Jia, Y.N. Wang, H. Gao, J.M. Ma, Gridded emission inventory of short–chain chlorinated paraffins and its validation in China, Environ. Pollut. 220 (2017) 132–141.
[45] U. Im, J.H. Christensen, O. Nielsen, M. Sand, R. Makkonen, C. Geels, C. Anderson, J. Kukkonen, S. Lopez-Aparicio, J. Brandt, Contributions of Nordic anthropogenic emissions on air pollution and premature mortality over the Nordic region and the Arctic, Atmos. Chem. Phys. 19 (2019) 12975–12992, https://doi.org/10.5194/acp-19-12975-2019.
[46] M. MacLeod, A.J. Fraser, D. Mackay, Evaluating and expressing the propagation of uncertainty in chemical fate and bioaccumulation models, Environ. Toxicol. Chem. 21 (4) (2002) 700–709, https://doi.org/10.1002/etc.5620210403.
[47] W.M. Jolly, M.A. Cochrane, P.H. Freeborn, Z.A. Holden, T.J. Brown, G.J. Williamson, D.M.J.S. Bowman, Climate-induced variations in global wildfire danger from 1979 to 2013, Nat. Commun. 6 (2015) 7537, https://doi.org/10.1038/ncomms8537.
[48] D.S. Ward, E. Shevliakova, S. Malyshev, S. Rabin, Trends and variability of global fire emissions due to historical anthropogenic activities, Global Biogeochem. Cycles 32 (2018) 122–142, https://doi.org/10.1002/2017GB005787.
[49] B. Zheng, P. Ciais, F. Chevallier, E. Chuvieco, Y. Chen, H. Yang, Increasing forest fire emissions despite the decline in global burned area, Sci. Adv. 7 (2021), eabh2646, https://doi.org/10.1126/sciadv.abh2646.
[50] S. Wu, S.W. Smith, J.S.H. Lee, Geophysical and anthropogenic drivers for global and regional fire emission trends from 2001 to 2019, Res. Square (2022), https://doi.org/10.21203/rs.3.rs-1537229/v1.
[51] V.I. Kharuk, M.L. Dvinskaya, S.T. Im, A.S. Golyukov, K.T. Smith, Wildfires in the siberian arctic, Fire 5 (2022) 106, https://doi.org/10.3390/fire5040106.
[52] Z. Zhang, L. Wang, N. Xue, Z. Du, Spatiotemporal analysis of active fires in the Arctic region during 2001–2019 and a fire risk assessment model, Fire 4 (3) (2021) 57, https://doi.org/10.3390/fire4030057.
[53] M.W. Jones, J.T. Abatzoglou, S. Veraverbeke, N. Andela, G. Lasslop, M. Forkel, A.J.P. Smith1, C. Burton, R.A. Betts, Gu.R. van der Werf, S. Sitch, J.G. Canadell, C. Santín, C. Kolden, S.H. Doerr, C. Le Quéré, Global and regional trends and drivers of fire under climate change, Rev. Geophys. 60 (2022), e2020RG000726, https://doi.org/10.1029/2020RG000726.
[54] C. Zarfl, M. Scheringer, M. Matthies, Screening criteria for long-range transport potential of organic substances in water, Environ. Sci. Technol. 45 (23) (2011) 10075–10081, https://doi.org/10.1021/es2012534.
[55] T.M. Lenton, J. Rockström, O. Gaffney, S. Rahmstorf, K. Richardson, W. Steffen, H.J. Schellnhuber, Climate tipping points - too risky to bet against, Nature 575 (2019) 592–595, https://doi.org/10.1038/d41586-019-03595-0.
[56] M. Fang, X. Li, H.W. Chen, D.L. Chen, Arctic amplification modulated by Atlantic Multidecadal Oscillation and greenhouse forcing on multidecadal to century scales, Nat. Commun. 13 (2022) 1865, https://doi.org/10.1038/s41467-022-29523-x.
[57] Q. Fan, X. Xua, S. He, B. Zhou, The extreme Arctic warm anomaly in November 2020, Atmos. Oceanogr. Sci. Libr. 15 (2022), 100260, https://doi.org/10.1016/j.aosl.2022.100260.
[58] Y. Wang, D. Hessen, B. Samset, F. Stordal, Evaluating global and regional land warming trends in the past decades with both MODIS and ERA5-Land land surface temperature data, Remote Sens. Environ. 280 (2022), 113181, https://doi.org/10.1016/j.rse.2022.113181.
[59] L. Zhang, J. Ma, C. Tian, Y. Li, H. Hung, Atmospheric transport of persistent semi-volatile organic chemicals to the Arctic and cold condensation in the mid-troposphere: Part 1: 2D modeling in mean atmosphere, Atmos. Chem. Phys. 10 (2010) 7303–7314, https://doi.org/10.5194/acp-10-7303-2010.
[60] Y. Shi, X. Liu, M. Wu, X. Zhao, Z. Ke, H. Brown, Relative importance of high-latitude local and long-range-transported dust for Arctic ice-nucleating particles and impacts on Arctic mixed-phase clouds, Atmos. Chem. Phys. 22 (2022) 2909–2935, https://doi.org/10.5194/acp-22-2909-2022.
[61] X. Chen, S. Kang, J. Yang, Investigation of distribution, transportation, and impact factors of atmospheric black carbon in the Arctic region based on a regional climate-chemistry model, Environ. Pollut. 257 (2020), 113127, https://doi.org/10.1016/j.envpol.2019.113127.
[62] T.J. Yasunari, H. Nakamura, K. Kim, N. Choi, M. Lee, Y. Tachibana, A.M. da Silva, Relationship between circum-Arctic atmospheric wave patterns and large-scale wildfires in boreal summer, Environ. Res. Lett. 16 (2021), 064009, https://doi.org/10.1088/1748-9326/abf7ef.
[63] T.W. Drake, S.E. Tank, A.V. Zhulidov, R.M. Holmes, T. Gurtovaya, R.G.M. Spencer, Increasing alkalinity export from large Russian Arctic rivers, Environ. Sci. Technol. 52 (2018) 8302–8308, https://doi.org/10.1021/acs.est.8b01051.
[64] X. Hu, H. Fan, M. Cai, S.A. Sejas, P. Taylor, S. Yang, A less cloudy picture of the inter-model spread in future global warming projections, Nat. Commun. 11 (2020) 4472, https://doi.org/10.1038/s41467-020-18227-9.